Optical Properties of Plasmonic Tunneling Junctions

Yuankai Tang and Hayk Harutyunyan*

Department of Physics, Emory University, Atlanta, GA 30322, United States

*email: hayk.harutyunyan@emory.edu

Abstract

Over the last century, quantum theories have revolutionized our understanding of material

properties. One of the most striking quantum phenomena occurring in heterogeneous media is the

quantum tunneling effect, where carriers can tunnel through potential barriers even if the barrier

height exceeds the carrier energy. Interestingly, the tunneling process can be accompanied by

absorption or emission of light. In most tunneling junctions made of noble metal electrodes these

optical phenomena are governed by plasmonic modes, i.e. light-driven collective oscillations of

surface electrons. In the emission process, plasmon excitation via inelastic tunneling electrons can

improve the efficiency of photon generation resulting in bright nanoscale optical sources. On the

other hand, the incident light can affect the tunneling behavior of plasmonic junctions as well,

leading to phenomena such as optical rectification and induced photocurrent. Thus, plasmonic

tunneling junctions provide a rich platform for investigating light-matter interactions paving the

way for various applications, including nanoscale light sources, sensors, and chemical reactors. In

this paper, we will introduce recent research progresses and promising applications based on the

plasmonic tunneling junctions.

1

1. Introduction

In quantum theory, a particle with energy E can penetrate through a potential barrier whose potential is higher than its own energy E. This is called the tunneling effect. According to the WKB approximation, its transmission probability is [1],

$$T = e^{-2\gamma} \tag{1}$$

where $\gamma = 1/\hbar \int_0^a |p(x)| \, dx$, a is the width of the barrier, and p is the momentum of the particle. An obvious consequence of this dependence is that the transmission probability decreases with the width and the height of the barrier. One of the most frequently encountered cases of tunneling effects is the electron tunneling between two materials. Typically, electrons can migrate from one electrode to another even if they are separated by a thin insulating layer. Due to the Fermi-Dirac distribution of the electron velocities inside of the electrodes, the tunneling current can be obtained by integrating the product of the transmission probability (Eq. 1) with the electron velocity distribution over the velocity range. The tunneling current density can be written as [2, 3]:

$$J = J_0 \left[\varphi e^{-A\sqrt{\varphi}} - (\varphi + eV) e^{-A\sqrt{\varphi + eV}} \right]$$
 (2)

where φ is the average potential barrier height, $J_0 = e/2\pi h(\beta \Delta s)^2$, $A = 4\pi\beta \Delta s/h\sqrt{2m}$, β is a correction factor, Δs is the width of the barrier at the starting point of the tunneling, and h is the Planck constant. The current density includes two exponential terms, which account for two opposite electron flows—the reflection and the transmission. Thus, the high bias voltages lowering the barrier height and the thinner insulators can be advantageous to realize tunneling resulting in larger current densities. In most practical situations, the thickness of insulator layers should be on the order of a few nanometers ($< \sim 5 \ nm$).

In many nanophotonic applications, tunneling junctions consist of noble metal electrodes, which can support generation of surface plasmons, typically in the form of gap modes. The excitation of strongly confined modes leads to a strong field enhancement due to the small mode volume, making them fascinating platforms to study light-matter interactions. The gap plasmons have been employed in many applications [4], such as strong plasmon-exciton coupling [5, 6], enhanced Raman scattering [7-9], fluorescence modifications [10], and nonlinear light generation [11, 12]. Combining plasmonic gap modes with tunneling junctions opens up a myriad of possibilities for exploring and tailoring the light-matter interactions as we discuss below.

Plasmonic gap modes can be excited by inelastic tunneling electrons as a byproduct of tunneling current generation in the nanometric junctions. The excited plasmons can couple to free-space modes resulting in the emission of light. Thus, a tunneling junction can be treated as a nanoscale light source, whose properties are determined by its materials' properties. Besides the traditional metal-insulator-metal tunneling junctions [3, 13-18], the inelastic tunneling and light emission have been realized in metal-insulator-semiconductor junctions [19, 20], metal-2D material junctions [21-24], and molecular junctions [25, 26].

A larger tunneling current typically provides a higher number of emitted photons. According to Eq. (2), a thinner insulating layer and a higher voltage could be beneficial for generating strong light emission. The limiting factors for such devices are related to the stability of the junction under the high voltages and physical limitations for fabricating tunnel gaps with decreasing thicknesses. Furthermore, the plasmonic properties start to diverge from the classical predictions in ultrathin gaps because of quantum effects. Specifically, the charge transfer effects diminish the field enhancement in the gaps due to the quenching of the near fields [7, 27, 28]. Although these effects on light generation in such small gaps are still not completely understood, a recent work has shown

that the light emission is indeed related to the charge-transfer modes in the ultrathin gaps [29]. However, these effects can usually be ignored because most experimental conditions involve tunneling junctions with thick enough insulator layers (>1 nm), that are not dominated by the charge-transfer modes.

The ability to tailor the properties of light-emitting plasmonic tunneling junctions is critical for achieving realistic applications. To that end, various configurations and geometric parameters have been explored. For instance, interference and diffraction of the propagating surface plasmon polaritons can be achieved in the tunneling junctions [30, 31]. Aperiodic groove arrays have been successfully used to control the surface plasmon polariton (SPP) propagation [32]. The spatial control of light emissions was realized in the alternating current (ac)-driven Al-AlO_x-Cu tunneling junctions with the changing barrier thicknesses [33]. Furthermore, in order to increase the light emission efficiency, considerable efforts have been dedicated to the optimization of the electron-to-photon conversion efficiency, including nanostructured optical antennas [3, 18, 21], rough electrode surfaces [34], and resonant tunneling junctions [35, 36].

On the other hand, incident light or excited plasmons can affect electronic properties of tunneling junctions as well. Photon-assisted tunneling and optical rectification have been realized in many experiments [37-43]. Similar to electric rectifiers, optical rectification can transfer ac signals to direct current (dc) signals. This transformation provides a method to detect ultrafast ac signals at optical frequencies, which are challenging to be measured directly due to their high frequencies. These phenomena that involve interactions between light and electronic excitations can be used to characterize properties of sub-nanometric gaps, such as near-field enhancement and temperature [38, 44, 45].

Besides direct applications of optically-active tunneling junctions based on light emission and absorption, these systems can be attractive for various other indirect applications. The emitted photons can be used to monitor the chemical reactions [46, 47], even at single-molecule levels [47]. Tunneling junctions encompassing molecules can work as solid-state molecular devices controlling charge transport [48, 49]. Finally, the electronic properties of the tunneling junctions can be treated as sensors and monitors to reveal physical processes [42, 43, 50-52].

In this perspective article, we will first discuss the light emission in junctions based on the inelastic tunneling, including its basic mechanisms, generation of plasmonic modes, optical antennas, and above-threshold light emission. Next, photon-assisted tunneling will be introduced, focusing on optical rectification, thermal effects, and photoemission. Finally, novel chemical applications based on the tunneling junctions will be reviewed.

2. Electroluminescence in plasmonic tunneling junctions

A nanoscale plasmonic light source can be realized using junctions which support inelastic electron tunneling. In general, the electroluminescence in the tunneling junctions can originate from two possible processes—inelastic tunneling (IET) and electron-hole recombination—dependent on the junctions' properties, such as their materials, geometries, and bias voltages [19]. In particular, electroluminescence can originate from electron-hole recombination in junctions including semiconductors, such as Si. According to Ref. [19], for Si/SiO2/Au junctions, electroluminescence is mainly dominated by the recombination of electrons and holes for Si with low doping level and by the quantum tunneling mechanism for Si with high doping level. Here, we will focus on the former process in the quantum tunneling regime.

Most common tunneling junctions consist of one or two metallic electrodes, typically noble metals, such as gold. These metal structures can support plasmonic modes, including gap modes and propagating modes. With the bias voltage applied on the junction, the quantum tunneling can occur between two electrodes, whose current-voltage (I-V) characteristics can be described by the Simmons model [2]. There are two kinds of tunneling electrons generated in this process—elastic tunneling electrons and inelastic tunneling electrons, as shown in Figure 1 (a). Due to energy conservation, it is obvious that elastic tunneling electrons do not lose energy and will not couple to the local density of optical states (LDOS), which is related to the density of electromagnetic modes in the volume and is proportional to the decay rate of a system [53]. In contrast, the inelastic tunneling electrons can be coupled to LDOS leading to the excitation of gap plasmons. Subsequently, the gap plasmons can couple to free-space radiation through some processes (Figure 1 (b)), which are dependent on the details of junctions. When the bias voltage exceeds the threshold that usually is a turning point in the Fowler-Nordheim representation [3], the tunneling regime will be established in the field emission leading to photon emission [3, 39]. Additionally, photons can be excited by inelastic tunneling electrons directly as well, however the efficiency of this mechanism is extremely low because of the momentum mismatch between photons and electrons $\lceil 14 \rceil$.

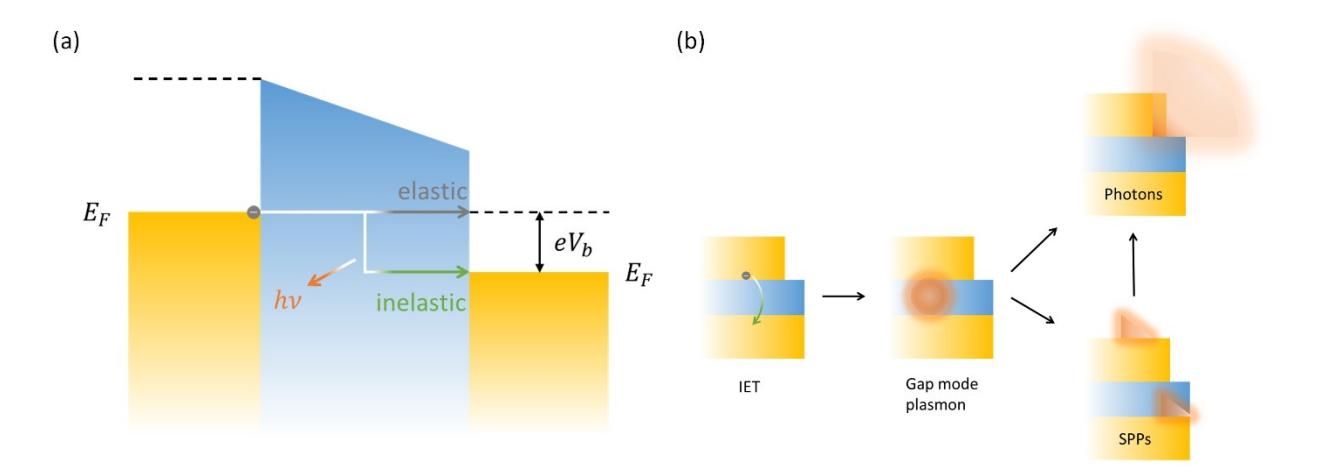


Figure 1 (a) Schematic of the tunneling process (b) Schematic of the electroluminescence processes in the tunneling junctions.

Parzefall and Novotny have previously summarized the inelastic tunneling mechanism and the efficiency of the electroluminescence providing a systematic guideline for these processes [54, 55]. Here, we briefly introduce this framework as a basis for the following discussions. The inelastic tunneling can be typically discussed in the context of three main theoretical approaches—energy-loss model, current fluctuation model, and spontaneous emission model [54, 55]. The latter model offers a connection between IET rate and LDOS ρ_{opt} and a suitable description of plasmon excitation in nanogaps [54, 55]. The IET rate can be calculated by integrating the spectral inelastic tunneling rate $\gamma_{inel}(\hbar\omega)$ over all energies $\Gamma_{inel}=\hbar\int_0^\infty \gamma_{inel}\left(\hbar\omega\right)d\omega$, where $\hbar\omega$ is the mode energy. In most cases, $\Gamma_{el}\gg\Gamma_{inel}$, therefore, without considering the optical properties of nanogaps the efficiency of IET in vacuum can be approximated as $\eta_{ele}=\left(\gamma_{inel}\left(\hbar\omega,\rho_{opt}=\rho_0\right)\right)/\Gamma_{el}$ where ρ_0 is the vacuum LDOS, which is called the source efficiency. This quantity is determined by the bias voltage, the gap distance, and the barrier height, however it is not dependent on optical properties of the system. Its efficiency is on the order of $10^{-8}eV^{-1}$, which is an extremely weak process [54].

The source efficiency of IET in vacuum is only dependent on the electronic properties of the nanogaps. However, IET needs to couple to the optical modes to excite plasmons in the tunneling gaps. Thus, the optical properties of the system play a significant role in the total source efficiency of IET due to the high LDOS in the tunneling junctions. The total electroluminescence efficiency η_{tot} includes three parts [54]:

$$\eta_{tot} = \eta_{ele} \times \eta_{opt} \times \eta_{em} \tag{3}$$

where η_{ele} is the ratio of the inelastic and elastic tunneling, $\eta_{opt} = \rho_{opt}/\rho_0$ is the ratio of the LDOS of the junction and the vacuum LDOS, and η_{em} is the outcoupling efficiency of the gap plasmons to surface plasmon polariton (SPP) or photons conversion. The second part is only dependent on the optical properties of the system. There are several contributions to the LDOS in the nanogaps, including gap plasmon modes, propagating plasmon modes (SPPs), and free photon modes. However, the LDOS of gap modes is several orders of magnitude higher than other contributions [54], which means that gap modes dominate the IET excitation process [54, 55]. Therefore, the free-space modes or the propagating modes are unlikely to be directly excited via IET. Eq. (3) implies that inelastic electrons are coupled to gap modes and omit the direct coupling of the inelastic tunneling electrons to free-space mode because the probability of the latter is extremely low. Most research studies focus on these three main factors to optimize the electroluminescence in the tunneling junctions.

2.1.Plasmons in the tunneling junctions

Although optically excited plasmons are more common in the recent literature, electron-excited modes trace their origin to the first observations of plasmonic phenomena in the 1950s [56]. This

was followed by the observation of light emission based on the inelastic tunneling two decades later [13]. More recently, this field has attracted renewed attention due to its promising applications as nanoscale optical devices [15, 25, 26].

As mentioned above, exciting gap modes is the necessary and crucial intermediate process to induce surface plasmon emission. In Ref. [14], a tunneling junction consisting of a smooth 20 nm gold film and a gold STM tip was used to observe the excitation of SPPs on a metal/air interface. Thus, the propagating modes were excited by dipole-like gap plasmon formed between the sharp tip and the film. However, the emission ring corresponding to the omnidirectional propagation of SPPs was replaced with a uniform emission pattern when the gold film is replaced by a 5nm granular gold film indicating that the increased surface roughness of the film leads to the disappearance of the propagating modes and their replacement with localized modes. It shows that gap modes excited by IET are indeed unable to outcouple to free space directly. Furthermore, a gold nanowire was used to separate the photon emission region from the tunneling junction region, as shown in Figure 2 (a). Photon emissions are detected successfully at the end of the nanowire, as shown in Figure 2 (b). Notwithstanding the low efficiency of only 5% due to the not optimal tunneling junction structure, these experiments demonstrated a clear pathway for energy conversion from electrons to photons and the potential for the development of electrically-driven nanoscale photon sources [14, 57].

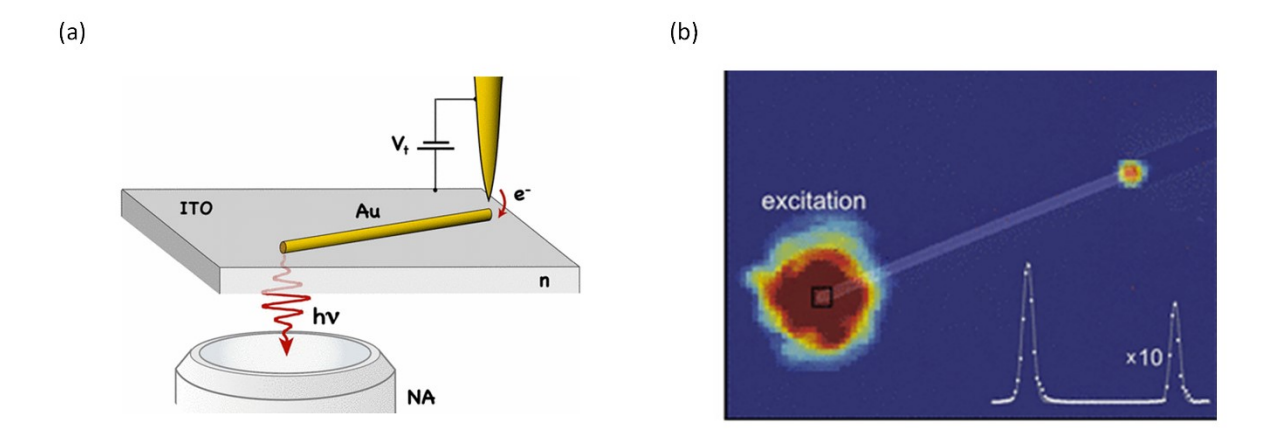


Figure 2 (a) Diagram of the experimental setup. (b) Photon emission map overlapped with the scanning electron microscope (SEM) image; Inset: emission intesity along the nanowire. [14] Copyright © 2011

American Physical Society.

However, there is not only one pathway for converting plasmons to free-space photons after the gap mode is excited. Ref. [34] shows three main paths to outcouple the gap modes in tunneling junctions: first, gap mode plasmons can be scattered into photons at the junction interfaces; second, gap modes can be coupled to propagating modes at the metal-dielectric interfaces; third, gap modes can be coupled to photon modes and propagating modes at the junction edge, as shown in Figure 3 (a-b). For example, the outcoupling route in Ref. [14] can be attributed to pathway 2, where gap plasmons are converted to propagating modes.

In addition, research has shown that the roughness of the gap has an important effect on its plasmonic properties [58]. The outcoupling efficiencies of tunnel junctions can be improved by the gap roughness, especially for the pathway 1, because of the roughness-induced momentum matching [34]. In Ref. [34], the outcoupling efficiency of Al-Al₂O₃-Au junctions is successfully raised to 0.62% by optimizing the electrode thickness and roughening the junction areas.

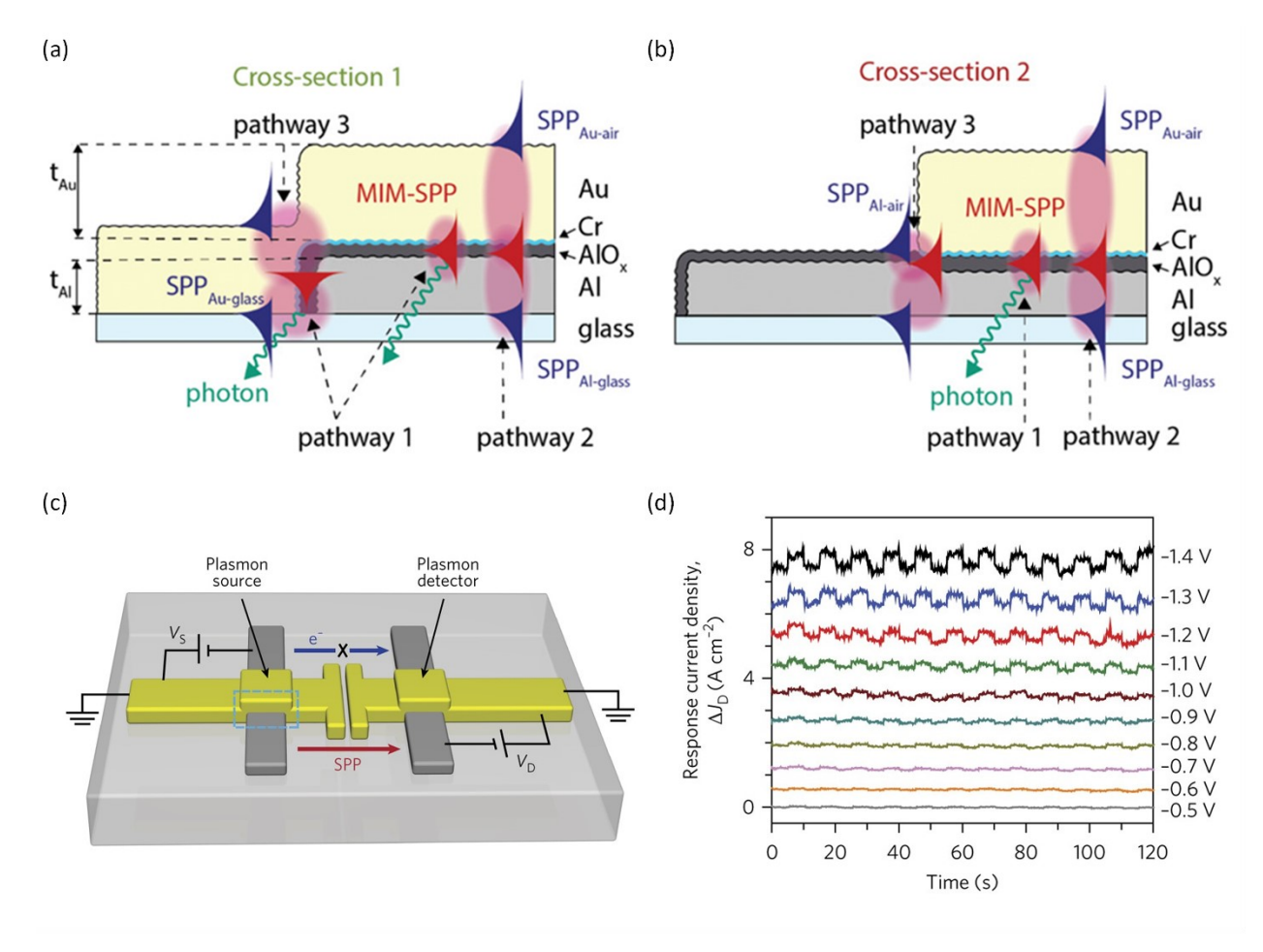


Figure 3 (a-b) Three outcoupling paths of gap plasmons in a Al-Al₂O₃-Au junction. [34] Copyright © 2020 The Authors. (c) Sketch of the source and detector tunneling junctions. (d) Response current densities as a function of the time with different bias voltages. [15] Copyright © 2017 The Authors

Most of electron-excited plasmons are detected by their accompanied light emissions in the tunneling junctions. However, they can also be sensed directly by tunneling currents without the plasmon-to-photon conversion. As shown in Figure 3 (c), this can be done using two adjacent tunneling junctions[15]. One of them is treated as a plasmonic source, and another one is treated as a detector. Similar to other tunneling mechanisms, the gap plasmons are excited in the source junction first, and then the gap mode couples to the propagating mode, which can cross over the gap between the two junctions. Finally, the propagating plasmons are detected by the right

tunneling junction via the optical rectification effect. The tunneling current of the detector junction can change with the presence of propagating plasmons as shown Figure 3 (d) [15].

2.2. Light emission based on tunneling junctions

Compared to the plasmonic source, the direct light emission source [3, 16-18, 21-23] is a much more attractive potential application based on the tunneling junction because of its compact size, ultrafast excitation time, and widely tunable emission wavelength. According to recent studies, three factors can affect the light emission rate—the electronic properties, the LDOS of the junction, and the output efficiency [54, 55].

Although roughening of the junctions mentioned above can improve the outcoupling efficiency, this approach will lead to saturation with increasing roughness [54]. Another method to increase the outcoupling efficiency is to optimize the geometry of electrodes in the junctions, by using optical antennas. Instead of using planar electrodes, gratings [59], nanoparticles [23], and nano antennas [3, 16, 18] can be employed as the electrodes in the tunneling gaps to improve the efficiencies by increasing both the LDOS and the outcoupling efficiency.

For example, a grating structure—gold periodical antenna—was used as the top-layer electrode in an Al-Al₂O₃-Au tunneling junction [59], as shown in Figure 4 (a). Its electron-to-photon efficiency can reach 1.6×10^{-6} photons per electron, which is 2700 times higher than the efficiency of the planar junction. Due to modified scattering cross sections, the antenna array significantly modifies the electroluminescence (EL) spectra compared to planar junctions, as shown in Figure 4 (b).

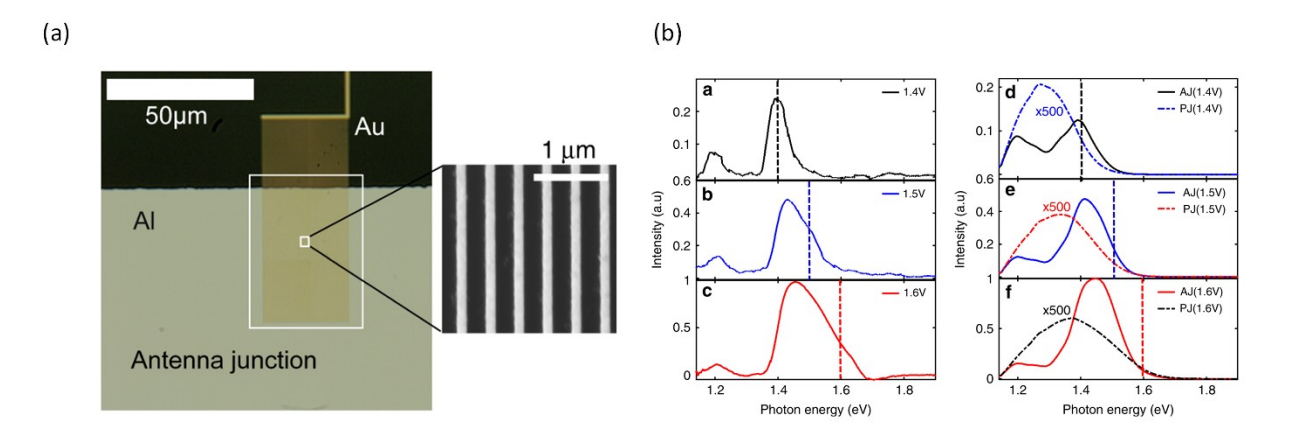


Figure 4 (a) Optical microscope and SEM images of a junction with grating structures. (b) Left: Experimental normalized EL spectra of the periodical antenna junctions with different bias voltages; Right: Theoretical normalized EL spectra of the periodical antenna junctions and the planar junction with different bias voltages. [59] Copyright © 2019 The Authors.

Similar to the grating nanostructures, a nano antenna with a nanoparticle in the gap was successfully used as a tunneling junction to emit light, as shown in Figure 5 (a) [3]. This structure not only can improve the electron-to-photon efficiency but can also provide a platform to modify the EL spectra by providing gap modes needed to couple to the free-space modes (photon modes) via scattering. As shown in Figure 5 (b), the scattering spectrum profiles with different geometries match the EL profiles well. Thus, the scattering cross sections of nano antennas can modify the EL spectra by changing the outcoupling efficiency. Furthermore, the cutoff frequencies of the EL spectra are limited by the bias voltages, which is evidence of the underlying inelastic tunneling mechanism. This nanostructure is utilized to realize nanoscale Yagi-Uda antennas [18], as shown in Figure 5 (c). These nanoscale antennas can provide a highly unidirectional emission in the optical regime with reflectors and directors, as shown in Figure 5 (d).

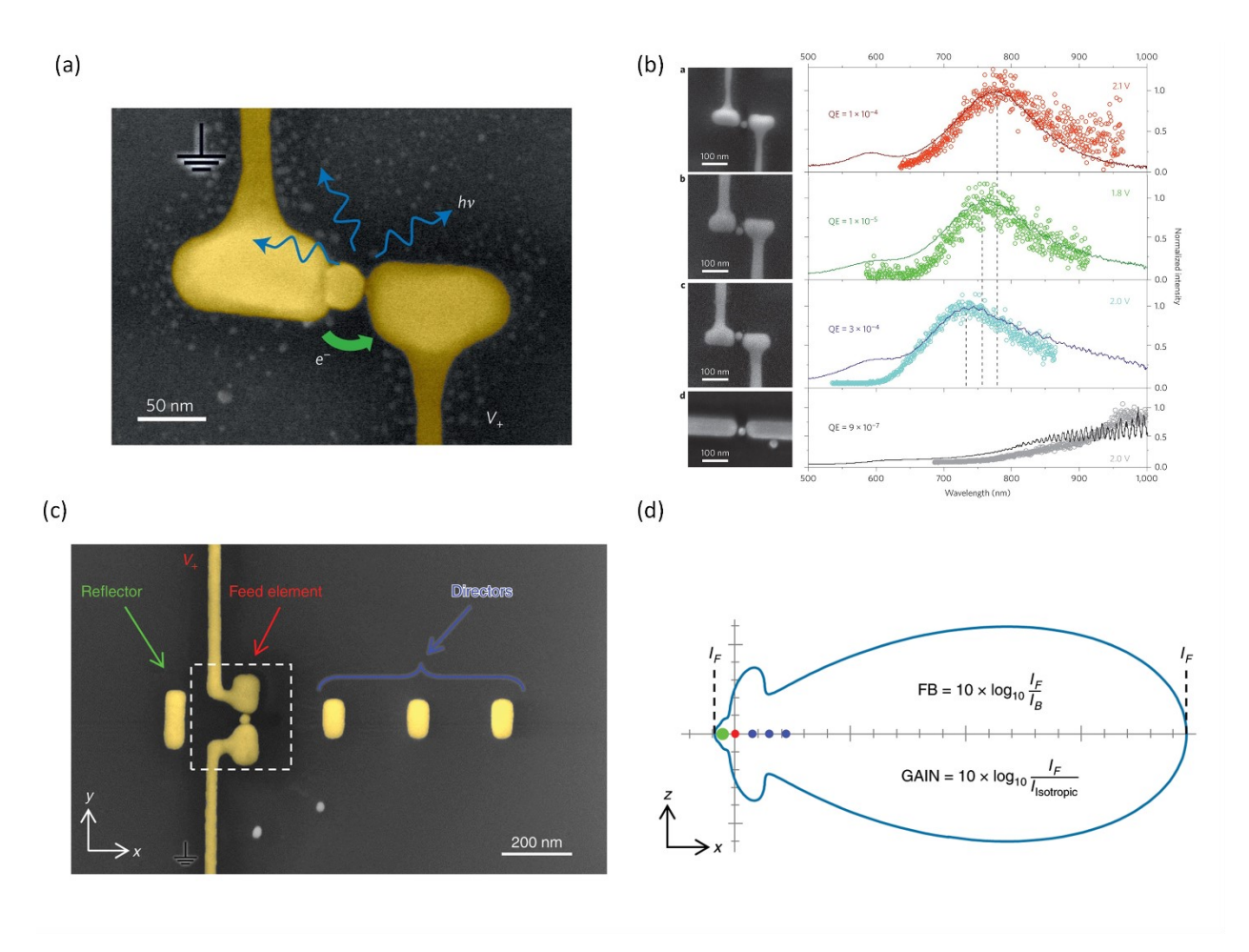


Figure 5 (a) SEM image of tunneling junctions. Nano antennas with different shapes are shwon in (b), left: SEM images; right: EL (open circles) and scattering spectra (solid lines). [3] Copyright © 2015 Nature Publishing Group. (c) SEM image of a Yagi-Uda antenna. (d) The highly unidirectional emission based on the simulation of the Yagi-Uda antenna. [18] Copyright © 2020, The Authors

The optical antennas' output efficiency is mostly dependent on their scattering cross sections. In the gaps, however, the LDOS sometimes does not exactly overlap with the scattering cross sections. This mismatch can lead to a low total output efficiency. As shown in Figure 6 (a-b), an optical antenna with two edge-to-edge silver cubes provides $(1.8 \pm 0.2) \times 10^{-3}$ external quantum efficiency when the scattering cross section is not matched with the LDOS [16]. With geometric optimizations, the external quantum efficiency finally increases by a factor of 10 and approaches 2% after the two are matched with each other, as shown Figure 6 (c).

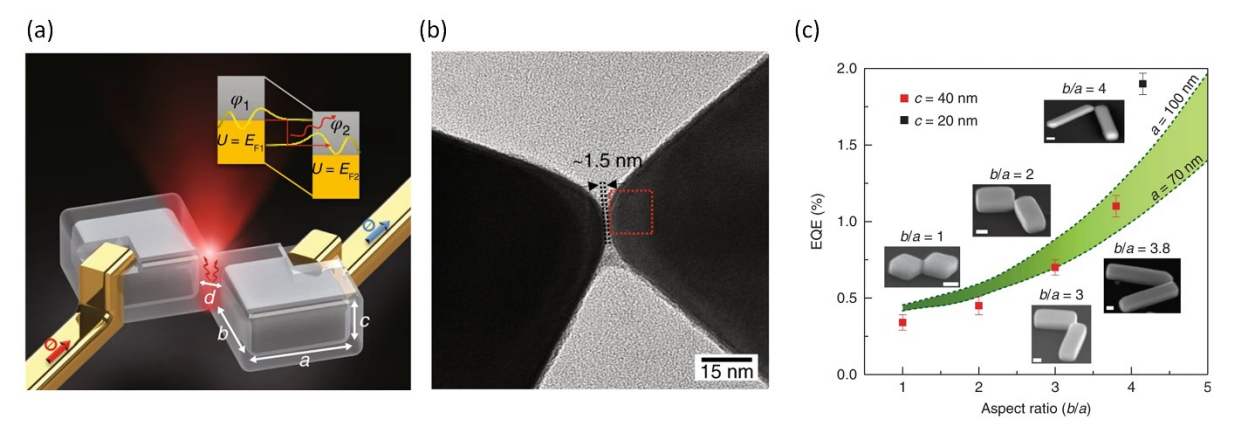


Figure 6 (a) Sketch of an edge-to-edge tunneling junction. (b) TEM image of the tunneling junction. (c) Simulated and experimental external quantum efficiency (EQE) of different nano antennas with different aspect ratios and heights (aspect ratio b/a, hight c). [16] Copyright © 2018, The Authors

Furthermore, 2D materials, including van der Waals materials, are widely used in tunneling optical antennas due to their special properties. For instance, hexagonal boron nitride (hBN) with its high potential barrier can be used as a robust insulator layer to support stable tunneling. In Ref. [21], the tunneling junctions are realized using Au-hBN-Au structures, as shown in Figure 7 (a). The nanoslots are fabricated on one of Au electrons with four separated sections to support different plasmonics modes. The emission profiles are determined by the transmittance spectra of these nanoslots and the intensities are improved due to the high outcoupling efficiencies. Simultaneously, the fast modulation of the light emission based on the inelastic tunneling was demonstrated in this work. In addition to the insulator, 2D materials can also be used as electrodes in the tunneling junctions. For example, graphene is a good conductor, which is routinely used as a top electrode with a Au bottom electrode and a hBN insulator, Figure 7 (c) [23]. In such structures, the plasmonic modes are not supported by the graphene electrode but the silver cubes on the top of the graphene coupled to the bottom Au layer. Similarly, the emission profiles are modified by the plasmonic modes.

Besides the optimization of the LDOS and the output efficiency, the first term in Eq. (3)—the electronic properties of the junction—can be used to enhance the electron-to-photon conversion efficiency as well, e.g. by using resonant tunneling structures. Recently, Qian et al. used metallic quantum well (MQW)-based tunnel junctions to realize the 30% external quantum efficiency [35]. This offers a step forward in the development of the tunneling junctions as compact plasmon /light sources.

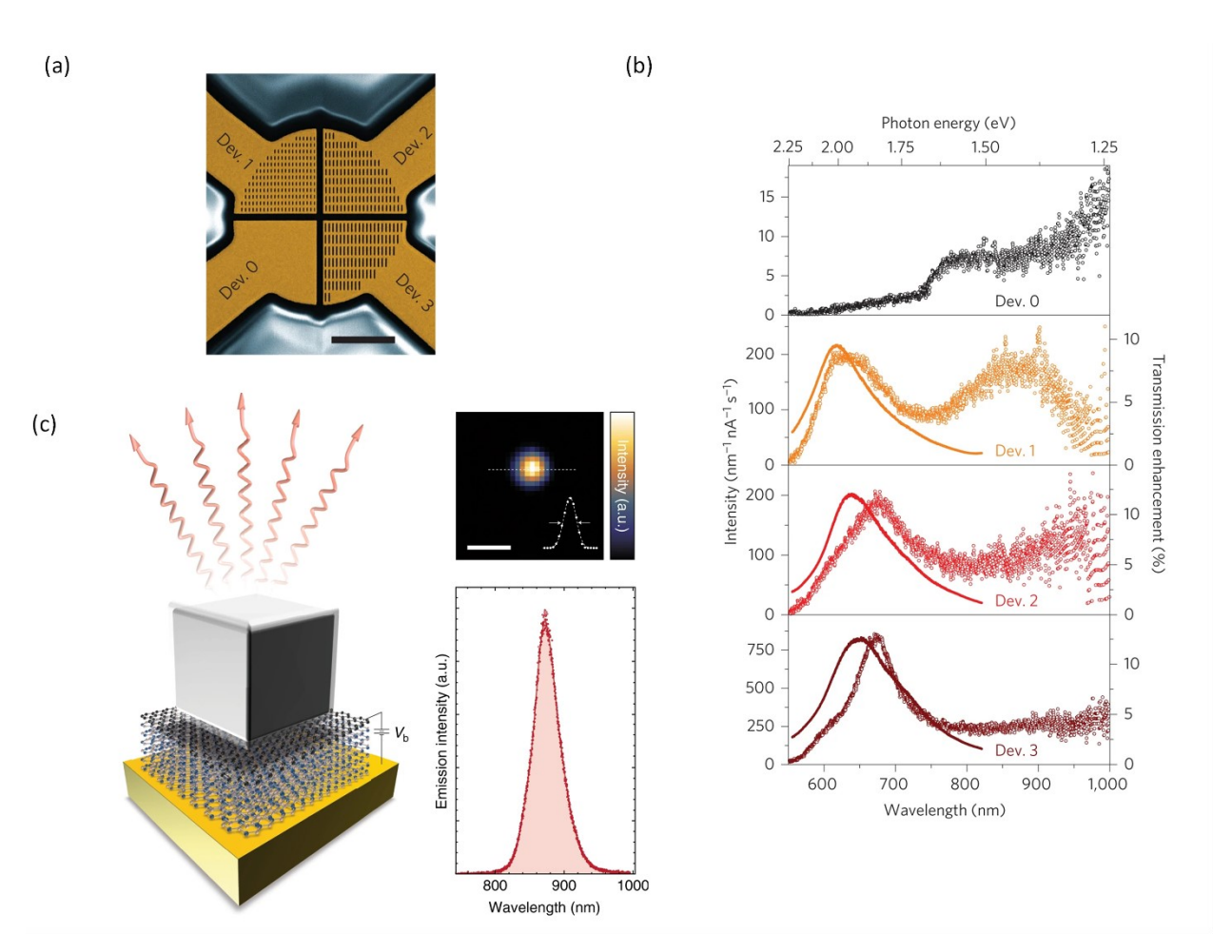


Figure 7 (a) SEM image of bottom electrodes with different slots for the tunneling junctions. (b) Emission spectra (open circle) and transmission enahncements (solid line) of these junctions. [21] Copyright © 2015, Nature Publishing Group (c) Left: Sketch of the tunneling junction consisting of the gold electrode, the hBN insulator layer, the graphene electrode, and the sliver nanocube. Right-top: Spatial distribution of

emitted ligth from a nanocube; Rigth-bottom: Emission spectra from a nanocube. [23] Copyright © 2019, The Authors

2.3. Above-threshold light emission based on the tunneling junctions

So far, we have discussed light emission in tunneling junctions with photon energies below the applied bias threshold. However, above-threshold light emission can be observed in tunneling junctions as well. The cut-off frequencies of the light emission excited by inelastic tunneling discussed above are limited by the bias voltages applied on the junction due to the energy conversion. However, the cut-off frequencies of the above-threshold light emission can be much higher than the energy of the inelastic electrons. The above-threshold light emission has been observed in the break junctions [60-62], where the electromigration method is used to fabricate ultranarrow gaps supporting tunneling [17, 39, 60, 61, 63, 64]. Buret et al. explain this emission behavior invoking spontaneous blackbody emission from hot electron gas thermalized by electron collisions [62]. Recently, other mechanisms based on hot carriers generated by nonradiative plasmonic decay [60] and electrons heated by plasmon decay at source electrodes [20], have been used to describe above-threshold light emission processes.

As shown in Figure 8 (a), a metallic electromigration break junction is used to support tunneling and emit photons [60]. Figure 8 (b) shows the Au/Cr junction's emission spectra, clearly showing that huge parts of the emitted light have energies higher than the maximum energy loss of the inelastic electrons. The pure gold junctions have the highest photon yield efficiency, compared to other lossy metals such as Cr and Pd. Thus, it was concluded that the light emission is indeed influenced by the plasmonic decay rate. The lossy metal can decrease the number of plasmons excited by the inelastic electrons and reduce the hot-carrier generation rate. In Figure 8 (c), it also

shows that the electron effective temperature T_{eff} is linearly increased with the bias voltages, $T_{eff} \propto V$, which is evidence of the plasmon-induced hot carrier generation [60]. In this mechanism, plasmons excited by inelastic tunneling electrons can induce hot electrons and hot holes via nonradiative decay, and recombination of these hot electrons and hot holes leads to above-threshold light emission, as shown in Figure 13 (d).

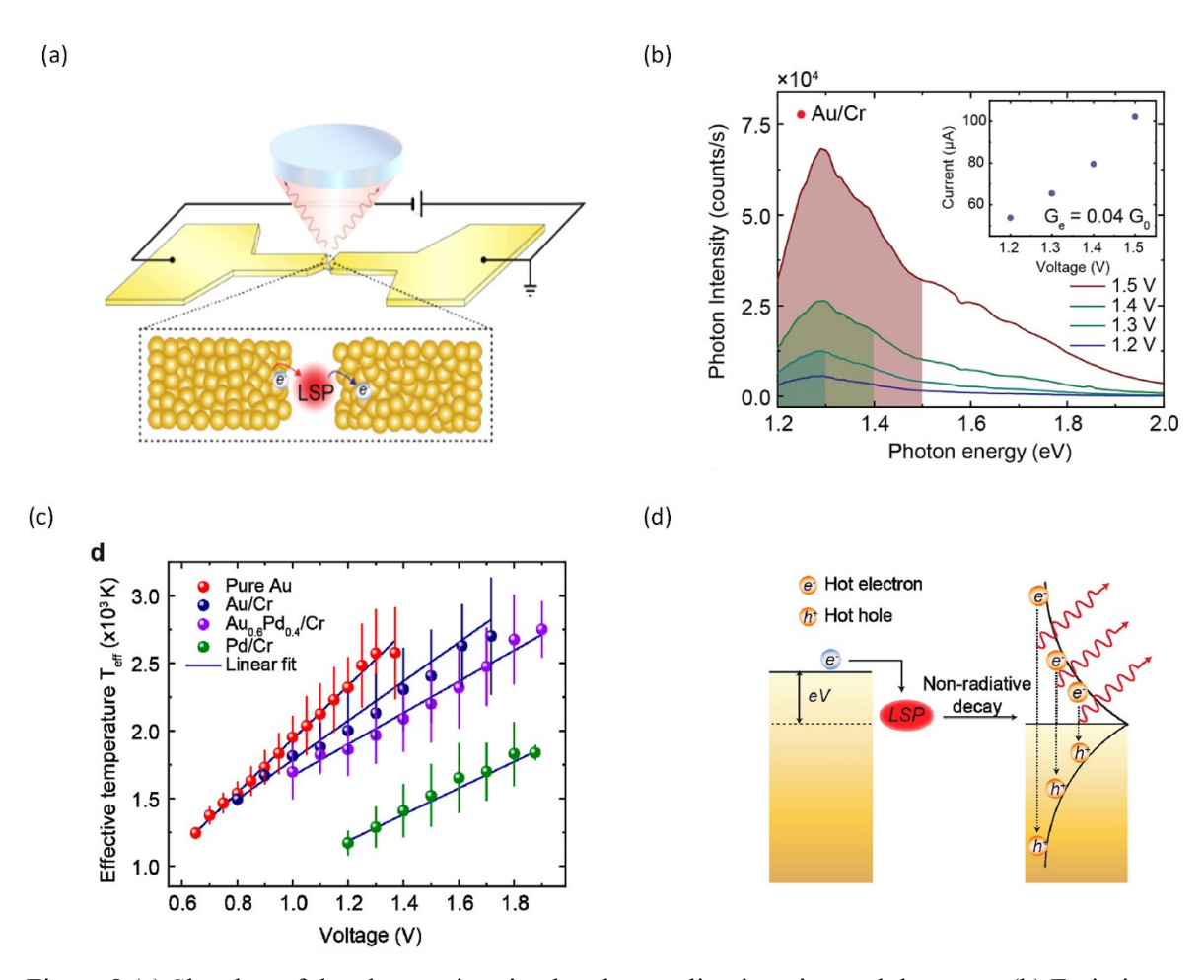


Figure 8 (a) Sketches of the electromigration break tunneling junction and the setup. (b) Emission spectra of the Au/Cr junction with different bias voltages. (c) Effective temperature as a function of the bias voltage for different junctions. (d) Sketch of the above-thershhold light emission mechanism [60]

Copyright © 2020 American Chemical Society

In Ref. [20], a metal-insulator-semiconductor structure is used to realize above-threshold emission, as shown in Figure 9 (a). Because the electrons flow from the metal to the semiconductor, this structure can rule out the possibility of heating electrons by tunneling or by plasmons in the drain. Comparing the emission spectra to the bias voltages, it is clear that parts of the emitted photons have energies higher than the threshold (eV_{bias}) , which are shaded in red in Figure 9 (b). To analyze the mechanism behind this phenomenon, this paper extracted the electron temperature from the spectra by fitting a Fermi-Dirac distribution. In Figure 9 (c), the effective temperature linearly increases with the applied bias when the voltage is lower than the plasmonic frequency. However, the increase slows down when the voltage is higher than the plasmonic frequency. The cut-off frequencies have similar trends. Thus, that plasmon indeed plays an important role in the above-threshold light emission and its mechanism is related to hot electrons based on the plasmonelectron interactions in the metal source electrode. Similarly, Shalem et al. claim that the energy of electron bath is proportional to the plasmon energy [20]. Although, both of these studies involve excitation of hot electrons via plasmon decay [20, 60], their light emission processes are considerably different from each other. In Cui et al., the above-threshold photons are generated via the recombination of hot electrons and hot holes [60]. In Shalem et al., however, the mechanism involves photon excitation through the inelastic tunneling of hot electrons.

The mechanism of the above-threshold light emission in plasmonic tunneling junctions is still not completely understood. However, it offers a novel approach for controlling light emission in tunneling junctions. Recently, for example, the above-threshold light emission was shown to increase by thousand times when the electromigration break junction was excited by both the tunneling electrons and the laser at the same time, as shown in the Figure 9 (d) [61].

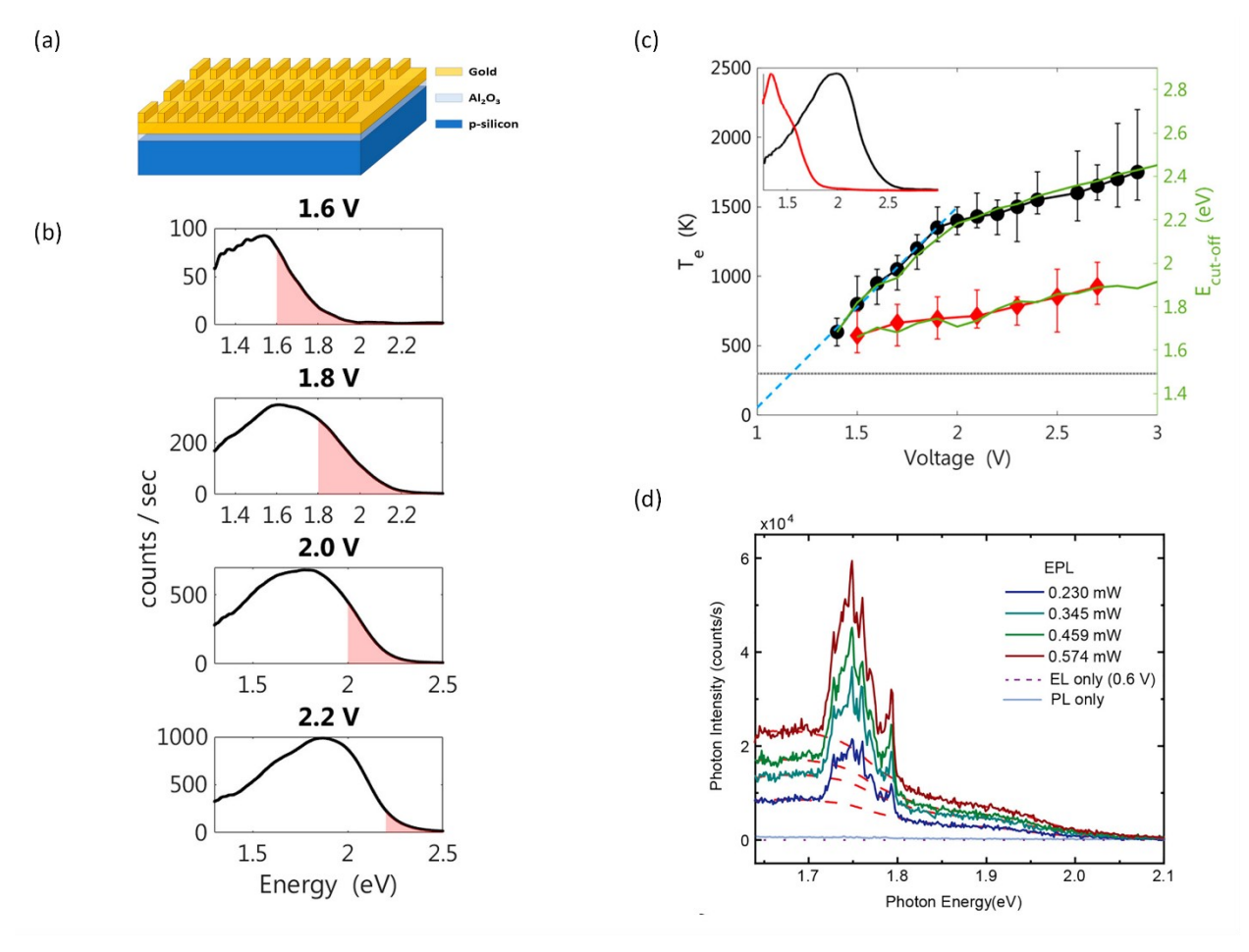


Figure 9 (a) Sketch of a metal-insulator-semiconductor (Au/Al₂O₃/p-type Si) tunneling junction. (b) Emssion spectra for different bias voltages. (c) Left axis: electon temperature as a function of the bias voltahes for two devices with different plamonic frequencies; right axis: cut-off energy as a function of the bias voltages. [20] Copyright © 2021 The Authors (d) Photon intensity as a function of the photon energy with the light and electronic exciation. [61] Copyright © 2021 American Chemical Society

3. Photon-assisted tunneling in plasmonic junctions

After considering light emission from plasmonic tunneling junctions in the previous section, here we will discuss a related phenomenon of photon-assisted tunneling, where the energy conversion is reversed resulting in current generation upon light absorption in tunnel junctions. The experimental observation and theoretical description of the photon-assisted tunneling have been first developed in 1960s, and the following research has generated considerable attention for decades, especially in the quantum dot systems and molecular junctions [65, 66]. Recently, the plasmonic properties of the junctions have also successfully been used to assist tunneling, due to their extremely large near fields and increased interaction cross sections [37-39].

When the tunneling junction is illuminated by a laser, the ac voltage induced on the junction via the optical fields with frequency ω can be expressed as $V_{opt}\cos(\omega t)$. Thus, its time-average tunneling current can be written as [37-39, 67]

$$I_{tot} = \sum_{n=-\infty}^{\infty} J_n^2 \left(\frac{eV_{opt}}{\hbar \omega} \right) I_{dc} \left(V_{dc} + \frac{n\hbar \omega}{e} \right). \tag{4}$$

where J_n is a Bessel function of the *n*th order, V_{dc} is the dc bias voltage, and V_{opt} is the amplitude of the optical voltage caused by the laser or plasmonic fields. According to Refs [37-39, 67], if the variance of the junction conductance is much slower than that of the optical voltage, the dc tunneling current can be approximated as

$$I_{tot} \approx I_{dc} \left(V_{dc}, V_{opt} = 0 \right) + \frac{1}{4} V_{opt}^2 \frac{\partial^2 I_{dc}}{\partial V_{dc}^2}$$
 (5)

by omitting the higher orders in Eq. (4). The first term of Eq. (5) is the regular tunneling current under the applied dc bias, and the second term is the photon-induced tunneling current which is typically called photocurrent. This mechanism is called optical rectification, which has been

observed in plasmonic tunneling junctions [37-39, 68]. The photocurrent is proportional to the nonlinear conductance and the intensity of the incident light.

3.1. Optical rectification

Ac tunneling caused by the incident light accompanies dc tunneling in many experimental configurations. However, the sensitivity and speed limitation of the measurement devices make it extremely challenging to detect the instantaneous ac quantum tunneling currents at optical frequencies. The time-average rectified dc tunneling currents can provide a chance to characterize the photon-induced tunneling behaviors [69]. The standard lock-in techniques are widely used in investigations of optical rectification to extract relationships between the photocurrent and the nonlinear conductance [37-39, 41].

A low capacitance junction can decrease the response time of the tunneling, which can be beneficial to the realization of the optical rectification. The electromigration method mentioned in the last section is a good approach for fabricating small tunneling junctions supporting optical rectification [37, 39, 70]. As shown in the left inset of Figure 10 (a), the electromigration break Au junctions were successfully employed to detect the optical rectification [37]. When the laser is incident on the gap area, the plasmons are excited leading to the appearance of a photocurrent. The signals extracted from the lock-in setups show that the photocurrent is almost the same as the nonlinear conductance term with the varying dc bias voltages in Figure 10 (a). Thus, the mechanism of the photocurrent generation can be identified as optical rectification. Simultaneously, as Figure 10 (b) shows, the photocurrent linearly increases with the incident laser power, which matches with the second term of Eq. (5) and is also evidence of the optical rectification.

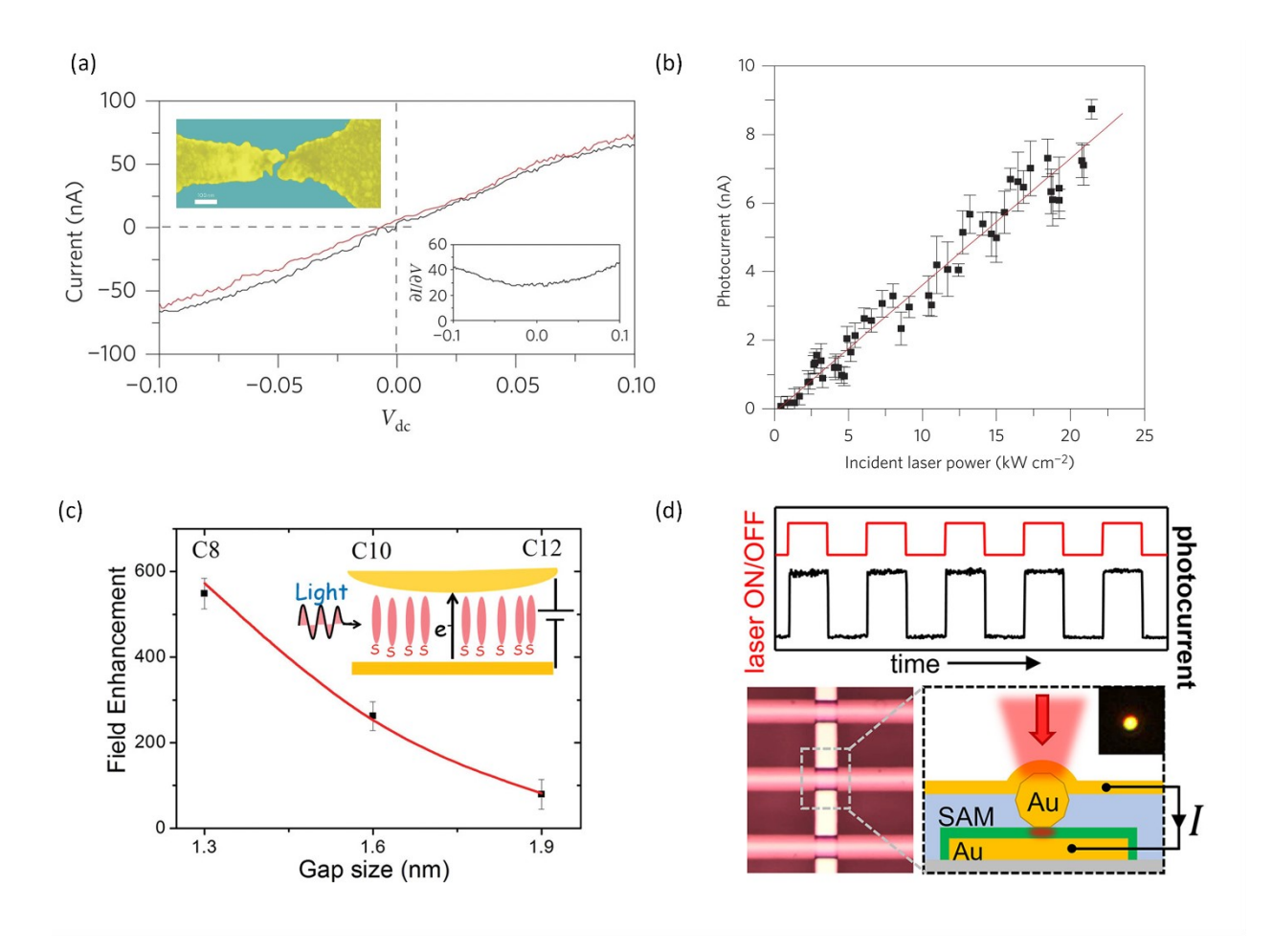


Figure 10 (a) Photocurrent (red line) and $1/4 \cdot V_{opt}^2 \cdot \partial^2 I_{dc}/\partial V_{dc}^2$ (black line) as a function of the dc bias voltage; Left inset: SEM image of the tunneling gap; Right inset: conductance as a function of the dc bias voltage. (b) Photocurrent as a function of incident laser power and the linear fitting line (red) [37] Copyright © 2010, Nature Publishing Group (c) Measured field enhancement in the tunneling gap as a function of the gap size; Inset: Diagram of the tunneling gap. [38] Copyright © 2011 American Chemical Society (d) Top: Laser signal and photocurrent as a function of time; Bottom: geometry of tunneling junctions. [41] Copyright © 2021 The Authors.

Molecule tunneling junctions are not only a good choice to realize rectification [71-74], but also are suitable for the observation of the effect in the optical regime, because of their well-defined and controllable gap sizes [38, 41]. Similar to the surface-enhanced Raman spectroscopy (SERS) used to probe molecules in the plasmonic gaps [7, 8, 10, 75, 76], the relationship between the photocurrent and the ac voltage can provide a method for detecting the plasmonic near fields in

the gaps. In Ref. [38], the Au plasmonic tunneling junctions with the embedded monolayer 1-octanethiol (C8), 1-decanethiol (C10), and 1-dodecanethiol (C12) molecules, are employed to realize optical rectification, as shown in the inset of Figure 10 (c). In this case, the gap distance is determined by the length of the molecules. Their I-V characteristics show that the photocurrent is proportional to the nonlinear conductance proving that the process is governed by optical rectification. The optical ac voltages V_{opt} can be extracted from the measurements, which are a measure of the near field enhancement in the plasmonic gaps compared to the incident free space power. Figure 10 (c) shows that the filed enhancement extracted from the photocurrent measurements decreases with the increasing gap size, which matches with simulation predications. Similarly, a self-assembled molecular monolayer (SAM) junction with gold electrodes can used for the optical rectification, with photocurrent being modulated by the incident light as shown in Figure 10 (d) [41].

According to Eq. (5) the photocurrent generation is expected to exhibit linear dependence on the incident power. However, this behavior can break down for powers above certain threshold. This scenario is explored in Ref. [39], where with the modest incident power, the photocurrent, the differential conductance, and the nonlinear conductance are enhanced accompanied with a strong SHG signal when the laser illuminates the gap (Figure 11 (c)). This behavior can again be described in the framework of optical rectification phenomenon. As shown in Figure 11 (a), the photocurrent initially shows linear behavior. However, for larger powers the dependence switches to third power, and finally to fifth power for even larger excitation powers. According to DFT calculations, these nonlinear photon-assisted tunneling effects can be attributed to d-Band electrons of Au, whose density of states and transition processes are shown in Figure 11 (b). When

the excitation power is large enough, the d-band electrons can be excited to the states near the Fermi level, leading to the nonlinear photocurrent via multiphoton absorptions.

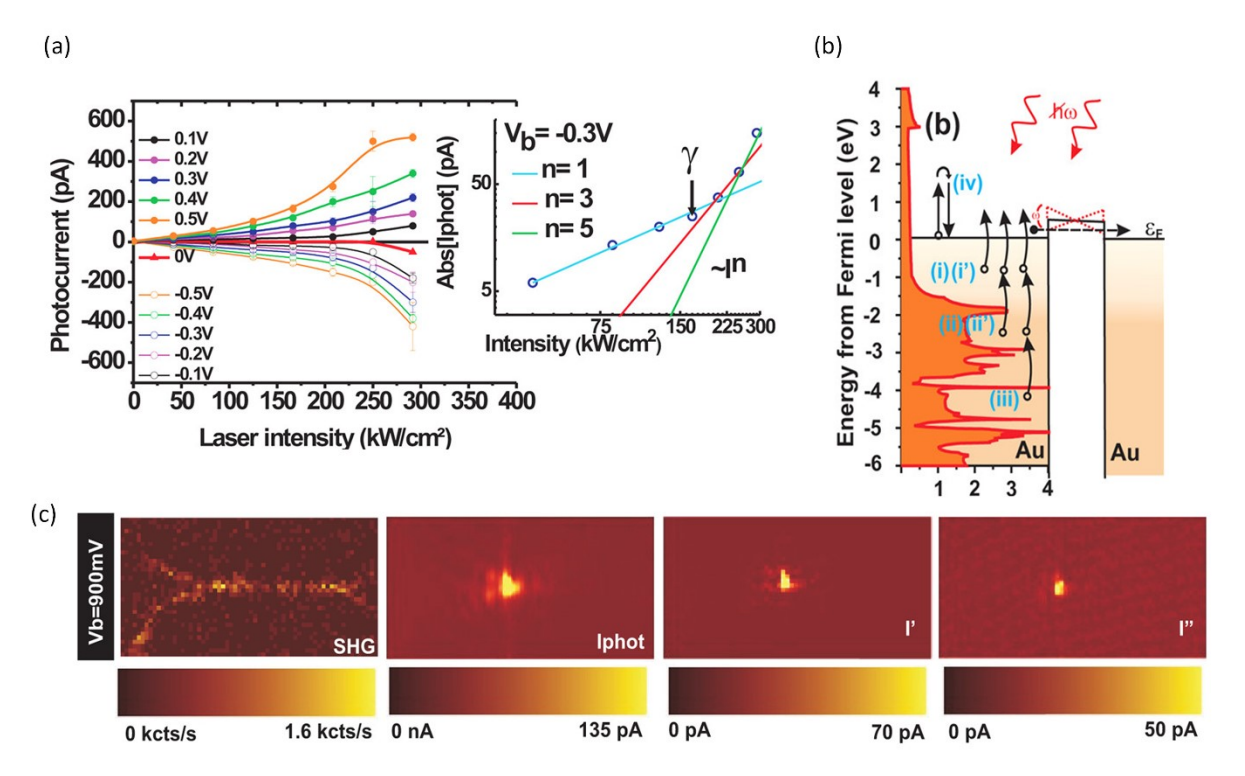


Figure 11 (a) Photocurrent as a function of laser intensity for different dc bias voltages. Inset: Fitting photocurrent and laser intensity by power law. (b) Calculated density of states and transition processes. (c) Scanning maps for SHG, photocurrent, conductance, and nonlinear conductance with 900 mV dc bias voltage. [39] Copyright © 2014 American Chemical Society

3.2. Other mechanisms contributing to currents in plasmonic tunneling junctions

Besides optical rectification, there are other phenomena induced by incident light, such as thermal effects and photoemission currents that can contribute to current generation in plasmonic tunneling junctions. Here, we will give a brief introduction of these interesting phenomena, which can provide additional avenues for manipulating the tunneling currents.

Although many investigations of optical rectification claim that thermal effects can be ignored due to their thick and symmetric plasmonic tunneling junctions [37-39], it should be noted that thermal

effects, such as thermal voltage and thermal expansion, caused by the incident light can also contribute to photon-assisted tunneling in some special conditions [45, 77-79]. For example, due to the thermal expansion, the resistance of the junction can decrease for suitable incident power, which causes the tunneling currents to increase [77].

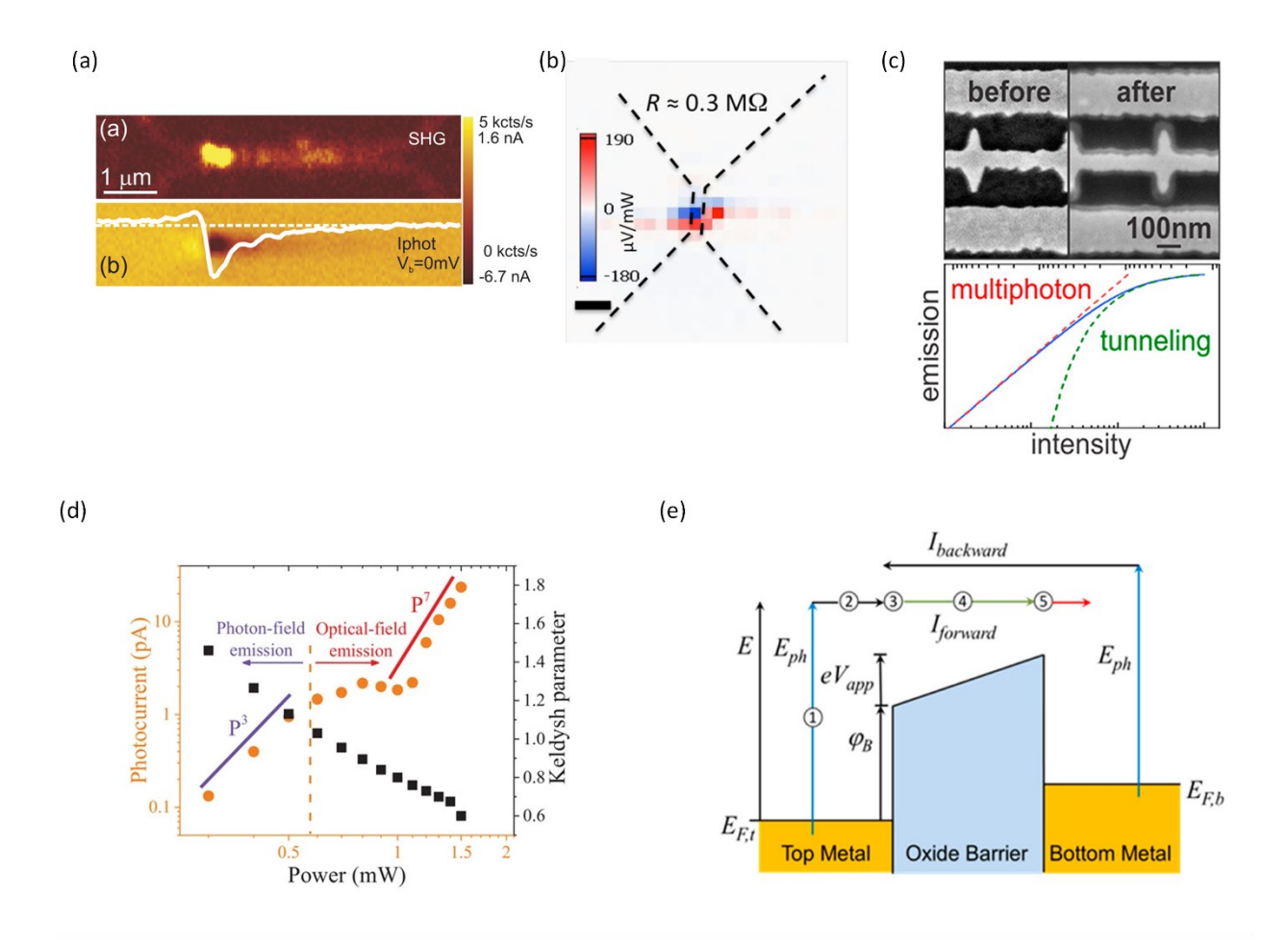


Figure 12 (a) SHG and photocurrent maps with 4MW/cm² laser. [39] Copyright © 2014 American Chemical Society (b) Photovoltage map of Ti-free Au nanogap. [78] Copyright © 2017 American Chemical Society (c) Top: SEM images of the nanojunctions before and after laser ablation. Bottom: Photoemission current as a function of incident intensity. [40] Copyright © 2019 American Chemical Society (d) Photocurrent and Keldysh parameter as a function of the incient power. [80] Copyright © 2021 The Authors (e) Sketch of hot electrons contributing to the current in a nanojunction. [81] Copyright © 2014 American Chemical Society

Ref. [39] observes the thermovoltage in the tunneling gaps when the incident power reaches 4MW/cm² which is much larger than the power (hundreds of kilowatts per square centimeter) used to realize nonlinear photo-assisted tunneling. Figure 12 (a) shows a photocurrent with different signs between two sides of the gap. The thermovoltage changes its sign when the laser illuminates the different sides of the gap leading to a temperature difference. Similar results are observed in Ref. [78], as shown in Figure 12 (b). When light is incident on a tunneling gap, a voltage difference is observed across the gap. It is claimed that the laser-induced voltage is caused by the electron energy-distribution differences between two sides of the gap, which is different from the conventional thermoelectric effect. Recently, Mennemanteuil et al. found both optical rectification and thermal effects contribute to the tunneling current [70]. Similarly, the changing I-V characteristics of the molecule junction can be used to detect the electronic and local lattice temperatures [45].

Photoemission caused by multiphoton absorption is another mechanism generating current in plasmonic tunneling junctions, although this cannot be classified as a "real" tunneling process as the electron energy can be higher the potential barrier. As shown in Figure 12 (c), the tunneling junctions are typically formed by laser ablation [40]. Zimmermann et al. find that the photocurrent is proportional to the 3.55 power of the squared laser field without bias voltage, which is characteristic for the photoemission process. According to the Keldysh theory, multiphoton absorption is believed to dominate the photoemission current for weak laser field [40]. For the strong laser field, their calculations show that the mechanism can turn into a tunneling process [40]. In Ref. [80], three steps of photocurrent are observed with the increasing laser power, as shown Figure 12 (d). For the lower power range, the photocurrent is proportional to the 3rd power order of the incident low power, which is believed to be caused by a hybrid mechanism, consisting

of a two-photon photoemission, one-photon-assisted tunneling, and direct tunneling [80]. For the medium power range, the photocurrent increases slowly with the power and even decreases, which can be attributed to the disturbed Schottky barrier. The final process shows a strong nonlinear behavior which is believed to be caused by the optical field-driven tunneling. Additionally, hot electrons excited by the laser can also generate a current in the plasmonic gap without the tunneling process, whose mechanism is described in Figure 12 (e) [81]. In conclusion, a plasmonic tunneling gap is a suitable platform to realize and monitor light-matter interactions due to its strong dependence on the near field enhancement and sensitive current.

4. Chemical applications based on plasmonic tunneling junctions

In previous sections, we have discussed two main categories of applications. The first was nanoscale light sources based on the inelastic tunneling. Second, applications based on the photo-assisted tunneling, such as nanoscale sensors, which can detect certain physical properties in the extremely small volumes with fast response times were discussed. As a final example, in this section we will introduce how plasmonic tunneling junctions can be used in chemical reactions.

Figure 13 (a) shows a plasmonic tunneling junction consisting of Au rods, Al₂O₃, a monolayer of poly-L-histidine (PLH), Ga₂O₃, and liquid eutectic gallium indium (EGaIn), where PLH is used as both a tunnel barrier and a reactant [47]. This tunneling junction can support both oxidation and reduction reactions related to O₂ and H₂ facilitated by hot electrons in the Au rods [47]. The interaction between O₂ molecules and hot electrons can accelerate the generation of transient negative O₂⁻ which finally becomes O atoms to oxidize Au. For the reduction reactions, the increased temperature via the relaxation of hot electrons can facilitate the reduction of Au oxides with H₂. Simultaneously, due to hot electrons H₂ molecules can be dissociated to H atoms which

can strongly reduce Au oxides. The hot electrons can be excited by both the elastic tunneling and the light excitation, although they have different effects on the reactions due to their different excitation power densities. With the low optical excitation power, plasmon-induced hot electrons cannot increase the temperature to facilitate the reduction of Au oxides. On the contrary, the tunneling-induced hot electrons can raise the temperature due to higher electric excitation power. Figure 13 (b) shows that the dc bias voltages have a strong influence on the reactions related to both O₂ and H₂, with higher voltages producing faster reaction rates. The chemical reactions driven by hot electrons are shown in Figure 13 (c), and oxidation of electrodes and barriers can change the electronic and optical properties of the junction leading the varying tunneling currents and emitted light. Thus, this junction can be used not only as a nanoreactor but also as a sensor.

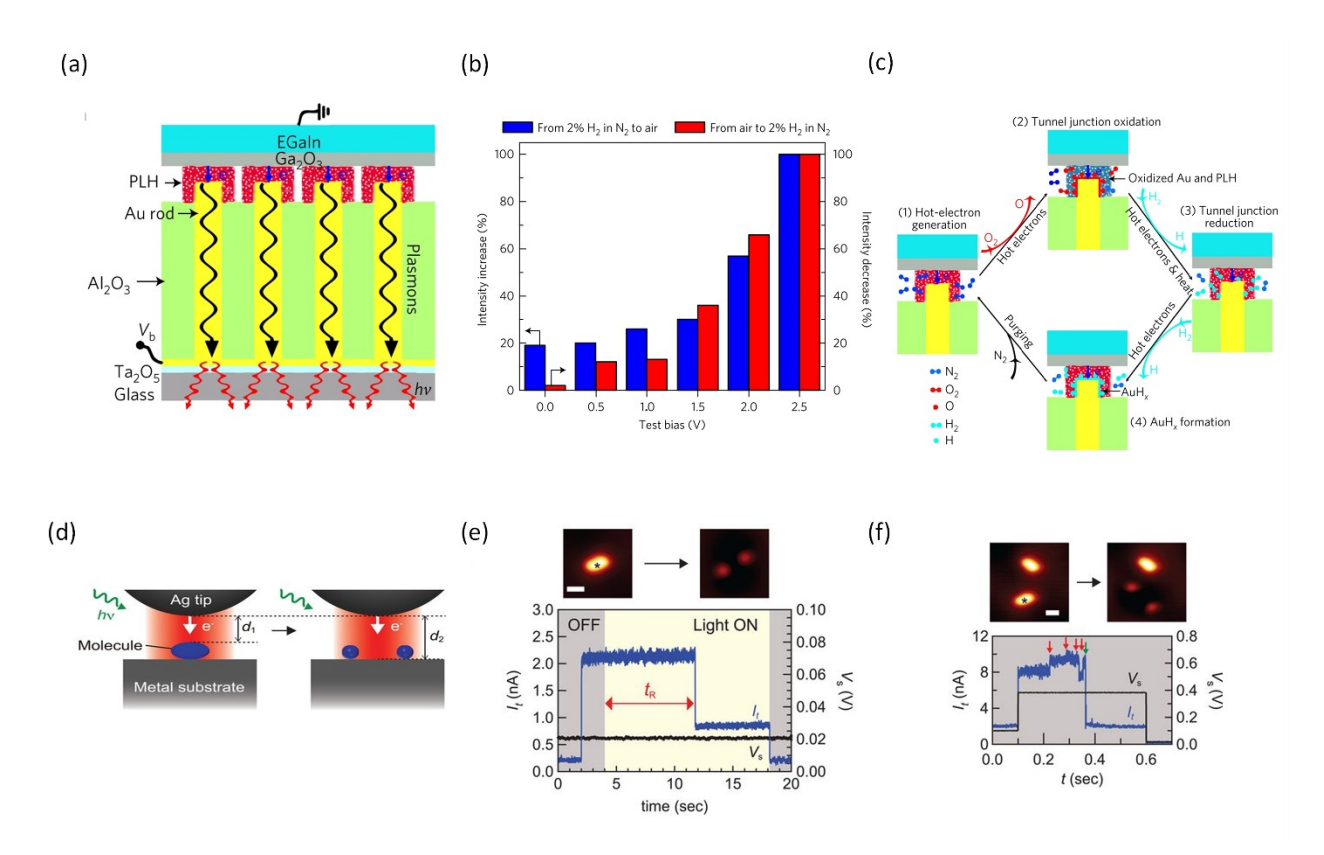


Figure 13 (a) Sketch of the tunneling gap used for chemical reactions. (b) Emission intensity changes as a function of bias voltages without incident ligth. (c) Processes of the chemical reactions in the tunneling junction. [47] Copyright © 2017, The Authors (d) Illustration of the real-time observation for chemical

reactions. (e) Top: STM images; Bottom: Tunneling current and bias voltage as a function of time with incident ligth. (f) Top: STM images; Bottom: Tunneling current and bias voltage as a function of time without incient ligth. Red arrow: rotation; Green arrow: dissociation. [46] Copyright © 2018 The Authors

Kazuma, et al. used tunneling currents and tunneling electrons in a scanning tunneling microscope (STM) to excite and monitor single-molecule chemical reactions in real time [46]. The dissociation reactions of Dimethyl disulfide (CH₃S)₂ can be induced by the strong field due to LSPR or injecting tunneling electrons. Due to the sensitivity of tunneling currents to the gap size, the tunneling current can reveal the changes of (CH₃S)₂ in the gap, as illustrated in Figure 13 (d). As shown in Figure 13 (e), the tunneling current with a low bias voltage, where the tunneling electrons with low energy cannot induce any reactions, shows the dissociation of (CH₃S)₂ when the incident light exciting plasmon leads to this chemical reaction. When the bias voltage increases, the energy of tunneling electrons is high enough to induce rotation and even dissociation reactions without light excitation. In this case, these processes can also be detected by the tunneling current in real time, as shown Figure 13 (e). In summary, plasmonic tunneling gaps offer a promising functionality to control and observe chemical reactions on the nanoscale.

5. Outlook

In this perspective article, we introduced the recent research and developments of plasmonic tunneling junctions, encompassing three main sections. First, we discussed the light emission via inelastic tunneling electrons in plasmonic tunneling gaps, which is an attractive photon source on the nanoscale. Due to the ultrafast process of tunneling, this light source can provide femtosecond response time. Various parameters of the tunneling junctions, including geometries, plasmonic

properties, electronic properties, and materials, can be modified to make the emitted light satisfy various experimental requirements. Furthermore, above threshold light emission can also be realized in plasmonic tunneling junctions providing a wider spectral range of emitted photons. Second, we focused on the light-induced currents in plasmonic tunneling junctions which show how the light-matter interactions in the nanogaps affect the tunneling phenomena, including optical rectification, thermal effects, and photoemission. These effects can be employed as detectors to reveal the physical properties of materials and processes in nanogaps. Finally, nanoscale reactors and sensors based on the plasmonic tunneling junctions were introduced. These can serve as promising platforms for chemical applications. Additionally, many related attractive phenomena and applications are not mentioned in this paper, such as the nonlinear light generation in tunneling gaps [82], energy harvesting based on optical rectifications [83], and tunneling switches [84]. In conclusion, all of these interesting phenomena and unique characteristics make the plasmonic tunneling junctions a promising field to study light-matter interaction on the nanoscale and to realize potential applications in the future.

Acknowledgments

This work was supported by National Science Foundation (CBET – 2231857).

References

- [1] D.J. Griffiths, D.F. Schroeter, Introduction to Quantum Mechanics, Cambridge University Press2018.
- [2] J.G. Simmons, Generalized Formula for the Electric Tunnel Effect between Similar Electrodes Separated by a Thin Insulating Film, Journal of Applied Physics, 34 (1963) 1793-1803.
- [3] J. Kern, R. Kullock, J. Prangsma, M. Emmerling, M. Kamp, B. Hecht, Electrically driven optical antennas, Nature Photonics, 9 (2015) 582-586.
- [4] J.J. Baumberg, J. Aizpurua, M.H. Mikkelsen, D.R. Smith, Extreme nanophotonics from ultrathin metallic gaps, Nature Materials, 18 (2019) 668-678.
- [5] R. Chikkaraddy, B. De Nijs, F. Benz, S.J. Barrow, O.A. Scherman, E. Rosta, A. Demetriadou, P. Fox, O. Hess, J.J. Baumberg, Single-molecule strong coupling at room temperature in plasmonic nanocavities, Nature, 535 (2016) 127-130.
- [6] K. Santhosh, O. Bitton, L. Chuntonov, G. Haran, Vacuum Rabi splitting in a plasmonic cavity at the single quantum emitter limit, Nature Communications, 7 (2016) ncomms11823.
- [7] W. Zhu, K.B. Crozier, Quantum mechanical limit to plasmonic enhancement as observed by surface-enhanced Raman scattering, Nature Communications, 5 (2014) 5228.
- [8] S.-Y. Ding, J. Yi, J.-F. Li, B. Ren, D.-Y. Wu, R. Panneerselvam, Z.-Q. Tian, Nanostructure-based plasmon-enhanced Raman spectroscopy for surface analysis of materials, Nature Reviews Materials, 1 (2016) 16021.
- [9] D.O. Sigle, S. Kasera, L.O. Herrmann, A. Palma, B. De Nijs, F. Benz, S. Mahajan, J.J. Baumberg, O.A. Scherman, Observing Single Molecules Complexing with Cucurbit[7]uril

- through Nanogap Surface-Enhanced Raman Spectroscopy, The Journal of Physical Chemistry Letters, 7 (2016) 704-710.
- [10] Y. Zhang, W. Chen, T. Fu, J. Sun, D. Zhang, Y. Li, S. Zhang, H. Xu, Simultaneous Surface-Enhanced Resonant Raman and Fluorescence Spectroscopy of Monolayer MoSe2: Determination of Ultrafast Decay Rates in Nanometer Dimension, Nano Letters, 19 (2019) 6284-6291.
- [11] J.B. Lassiter, X. Chen, X. Liu, C. Ciracì, T.B. Hoang, S. Larouche, S.-H. Oh, M.H. Mikkelsen, D.R. Smith, Third-Harmonic Generation Enhancement by Film-Coupled Plasmonic Stripe Resonators, ACS Photonics, 1 (2014) 1212-1217.
- [12] F. Wang, A.B.F. Martinson, H. Harutyunyan, Efficient Nonlinear Metasurface Based on Nonplanar Plasmonic Nanocavities, ACS Photonics, 4 (2017) 1188-1194.
- [13] J. Lambe, S.L. Mccarthy, Light Emission from Inelastic Electron Tunneling, Physical Review Letters, 37 (1976) 923-925.
- [14] P. Bharadwaj, A. Bouhelier, L. Novotny, Electrical Excitation of Surface Plasmons, Physical Review Letters, 106 (2011).
- [15] W. Du, T. Wang, H.-S. Chu, C.A. Nijhuis, Highly efficient on-chip direct electronic—plasmonic transducers, Nature Photonics, 11 (2017) 623-627.
- [16] H. Qian, S.-W. Hsu, K. Gurunatha, C.T. Riley, J. Zhao, D. Lu, A.R. Tao, Z. Liu, Efficient light generation from enhanced inelastic electron tunnelling, Nature Photonics, 12 (2018) 485-488.
- [17] J. Qin, Y. Liu, H. Luo, Z. Jiang, W. Cai, L. Wang, Tunable Light Emission by Electrically Excited Plasmonic Antenna, ACS Photonics, 6 (2019) 2392-2396.

- [18] R. Kullock, M. Ochs, P. Grimm, M. Emmerling, B. Hecht, Electrically-driven Yagi-Uda antennas for light, Nature Communications, 11 (2020).
- [19] F. Wang, Y. Liu, T.J. Duffin, V. Kalathingal, S. Gao, W. Hu, Y. Guo, S.-J. Chua, C.A. Nijhuis, Silicon-Based Quantum Mechanical Tunnel Junction for Plasmon Excitation from Low-Energy Electron Tunneling, ACS Photonics, 8 (2021) 1951-1960.
- [20] G. Shalem, O. Erez-Cohen, D. Mahalu, I. Bar-Joseph, Light Emission in Metal–Semiconductor Tunnel Junctions: Direct Evidence for Electron Heating by Plasmon Decay, Nano Letters, 21 (2021) 1282-1287.
- [21] M. Parzefall, P. Bharadwaj, A. Jain, T. Taniguchi, K. Watanabe, L. Novotny, Antenna-coupled photon emission from hexagonal boron nitride tunnel junctions, Nature Nanotechnology, 10 (2015) 1058-1063.
- [22] S. Namgung, D.A. Mohr, D. Yoo, P. Bharadwaj, S.J. Koester, S.-H. Oh, Ultrasmall Plasmonic Single Nanoparticle Light Source Driven by a Graphene Tunnel Junction, ACS Nano, 12 (2018) 2780-2788.
- [23] M. Parzefall, Á. Szabó, T. Taniguchi, K. Watanabe, M. Luisier, L. Novotny, Light from van der Waals quantum tunneling devices, Nature Communications, 10 (2019).
- [24] Z. Wang, V. Kalathingal, T.X. Hoang, H.-S. Chu, C.A. Nijhuis, Optical Anisotropy in van der Waals materials: Impact on Direct Excitation of Plasmons and Photons by Quantum Tunneling, Light: Science & Applications, 10 (2021).
- [25] X. He, J. Tang, H. Hu, J. Shi, Z. Guan, S. Zhang, H. Xu, Electrically Driven Highly Tunable Cavity Plasmons, ACS Photonics, 6 (2019) 823-829.

- [26] W. Du, T. Wang, H.-S. Chu, L. Wu, R. Liu, S. Sun, W.K. Phua, L. Wang, N. Tomczak, C.A. Nijhuis, On-chip molecular electronic plasmon sources based on self-assembled monolayer tunnel junctions, Nature Photonics, 10 (2016) 274-280.
- [27] W. Zhu, R. Esteban, A.G. Borisov, J.J. Baumberg, P. Nordlander, H.J. Lezec, J. Aizpurua, K.B. Crozier, Quantum mechanical effects in plasmonic structures with subnanometre gaps, Nature Communications, 7 (2016) 11495.
- [28] G. Hajisalem, M.S. Nezami, R. Gordon, Probing the Quantum Tunneling Limit of Plasmonic Enhancement by Third Harmonic Generation, Nano Letters, 14 (2014) 6651-6654.
- [29] A.L. Paoletta, E.-D. Fung, L. Venkataraman, Gap Size-Dependent Plasmonic Enhancement in Electroluminescent Tunnel Junctions, ACS Photonics, 9 (2022) 688-693.
- [30] A. Radulescu, V. Kalathingal, Z. Wang, C.A. Nijhuis, Coherence Between Different Propagating Surface Plasmon Polariton Modes Excited by Quantum Mechanical Tunnel Junctions, Advanced Optical Materials, 10 (2022) 2101804.
- [31] A. Radulescu, V. Kalathingal, C.A. Nijhuis, Geometric Control Over the Edge Diffraction of Electrically Excited Surface Plasmon Polaritons by Tunnel Junctions, ACS Photonics, 8 (2021) 3591-3598.
- [32] Y. Lin, T.X. Hoang, H.-S. Chu, C.A. Nijhuis, Directional launching of surface plasmon polaritons by electrically driven aperiodic groove array reflectors, Nanophotonics, 10 (2021) 1145-1154.

- [33] F. Wang, T.X. Hoang, H.S. Chu, C.A. Nijhuis, Spatial Control over Stable Light-Emission from AC-Driven CMOS-Compatible Quantum Mechanical Tunnel Junctions, Laser & Photonics Reviews, 16 (2022) 2100419.
- [34] K.S. Makarenko, T.X. Hoang, T.J. Duffin, A. Radulescu, V. Kalathingal, H.J. Lezec, H.S. Chu, C.A. Nijhuis, Efficient Surface Plasmon Polariton Excitation and Control over Outcoupling Mechanisms in Metal–Insulator–Metal Tunneling Junctions, Advanced Science, 7 (2020) 1900291.
- [35] H. Qian, S. Li, S.-W. Hsu, C.-F. Chen, F. Tian, A.R. Tao, Z. Liu, Highly-efficient electrically-driven localized surface plasmon source enabled by resonant inelastic electron tunneling, Nature Communications, 12 (2021).
- [36] A.V. Uskov, J.B. Khurgin, I.E. Protsenko, I.V. Smetanin, A. Bouhelier, Excitation of plasmonic nanoantennas by nonresonant and resonant electron tunnelling, Nanoscale, 8 (2016) 14573-14579.
- [37] D.R. Ward, F. Hüser, F. Pauly, J.C. Cuevas, D. Natelson, Optical rectification and field enhancement in a plasmonic nanogap, Nature Nanotechnology, 5 (2010) 732-736.
- [38] R. Arielly, A. Ofarim, G. Noy, Y. Selzer, Accurate Determination of Plasmonic Fields in Molecular Junctions by Current Rectification at Optical Frequencies, Nano Letters, 11 (2011) 2968-2972.
- [39] A. Stolz, J. Berthelot, M.-M. Mennemanteuil, G. Colas Des Francs, L. Markey, V. Meunier, A. Bouhelier, Nonlinear Photon-Assisted Tunneling Transport in Optical Gap Antennas, Nano Letters, 14 (2014) 2330-2338.

- [40] P. Zimmermann, A. Hötger, N. Fernandez, A. Nolinder, K. Müller, J.J. Finley, A.W. Holleitner, Toward Plasmonic Tunnel Gaps for Nanoscale Photoemission Currents by On-Chip Laser Ablation, Nano Letters, 19 (2019) 1172-1178.
- [41] D. Kos, D.R. Assumpcao, C. Guo, J.J. Baumberg, Quantum Tunneling Induced Optical Rectification and Plasmon-Enhanced Photocurrent in Nanocavity Molecular Junctions, ACS Nano, 15 (2021) 14535-14543.
- [42] Q. Zou, X. Chen, Y. Zhou, X. Jin, Z. Zhang, J. Qiu, R. Wang, W. Hong, J. Su, D.-H. Qu, H. Tian, Photoconductance from the Bent-to-Planar Photocycle between Ground and Excited States in Single-Molecule Junctions, Journal of the American Chemical Society, 144 (2022) 10042-10052.
- [43] Y. Selzer, Elucidating the Contributions of Plasmon-Induced Excitons and Hot Carriers to the Photocurrent of Molecular Junctions, The Journal of Physical Chemistry C, 124 (2020) 8680-8688.
- [44] H. Bi, C. Jing, P. Hasch, Y. Gong, D. Gerster, J.V. Barth, J. Reichert, Single Molecules in Strong Optical Fields: A Variable-Temperature Molecular Junction Spectroscopy Setup, Analytical Chemistry, 93 (2021) 9853-9859.
- [45] N. Nachman, Y. Selzer, Thermometry of Plasmonic Heating by Inelastic Electron Tunneling Spectroscopy (IETS), Nano Letters, 17 (2017) 5855-5861.
- [46] E. Kazuma, J. Jung, H. Ueba, M. Trenary, Y. Kim, Real-space and real-time observation of a plasmon-induced chemical reaction of a single molecule, Science, 360 (2018) 521-525.
- [47] P. Wang, A.V. Krasavin, M.E. Nasir, W. Dickson, A.V. Zayats, Reactive tunnel junctions in electrically driven plasmonic nanorod metamaterials, Nature Nanotechnology, 13 (2018) 159-164.

- [48] B. Han, Y. Li, X. Ji, X. Song, S. Ding, B. Li, H. Khalid, Y. Zhang, X. Xu, L. Tian, H. Dong, X. Yu, W. Hu, Systematic Modulation of Charge Transport in Molecular Devices through Facile Control of Molecule–Electrode Coupling Using a Double Self-Assembled Monolayer Nanowire Junction, Journal of the American Chemical Society, DOI 10.1021/jacs.0c02215(2020).
- [49] R. Gupta, P. Jash, P. Sachan, A. Bayat, V. Singh, P.C. Mondal, Electrochemical Potential-Driven High-Throughput Molecular Electronic and Spintronic Devices: From Molecules to Applications, Angewandte Chemie International Edition, 60 (2021) 26904-26921.
- [50] X. Chen, C.A. Nijhuis, The Unusual Dielectric Response of Large Area Molecular Tunnel Junctions Probed with Impedance Spectroscopy, Advanced Electronic Materials, 8 (2022) 2100495.
- [51] P. Gehring, J.M. Thijssen, H.S.J. Van Der Zant, Single-molecule quantum-transport phenomena in break junctions, Nature Reviews Physics, 1 (2019) 381-396.
- [52] L. Xue, H. Yamazaki, R. Ren, M. Wanunu, A.P. Ivanov, J.B. Edel, Solid-state nanopore sensors, Nature Reviews Materials, 5 (2020) 931-951.
- [53] L. Novotny, B. Hecht, Principles of nano-optics, Cambridge university press2012.
- [54] M. Parzefall, L. Novotny, Light at the End of the Tunnel, ACS Photonics, 5 (2018) 4195-4202.
- [55] M. Parzefall, L. Novotny, Optical antennas driven by quantum tunneling: a key issues review, Reports on Progress in Physics, 82 (2019) 112401.
- [56] S.A. Maier, Plasmonics: fundamentals and applications, Springer Science & Business Media2007.

- [57] T. Wang, E. Boer-Duchemin, Y. Zhang, G. Comtet, G. Dujardin, Excitation of propagating surface plasmons with a scanning tunnelling microscope, Nanotechnology, 22 (2011) 6.
- [58] C. Ciracì, F. Vidal-Codina, D. Yoo, J. Peraire, S.-H. Oh, D.R. Smith, Impact of Surface Roughness in Nanogap Plasmonic Systems, ACS Photonics, 7 (2020) 908-913.
- [59] C. Zhang, J.-P. Hugonin, A.-L. Coutrot, C. Sauvan, F. Marquier, J.-J. Greffet, Antenna surface plasmon emission by inelastic tunneling, Nature Communications, 10 (2019).
- [60] L. Cui, Y. Zhu, M. Abbasi, A. Ahmadivand, B. Gerislioglu, P. Nordlander, D. Natelson, Electrically Driven Hot-Carrier Generation and Above-Threshold Light Emission in Plasmonic Tunnel Junctions, Nano Letters, 20 (2020) 6067-6075.
- [61] L. Cui, Y. Zhu, P. Nordlander, M. Di Ventra, D. Natelson, Thousand-fold Increase in Plasmonic Light Emission via Combined Electronic and Optical Excitations, Nano Letters, 21 (2021) 2658-2665.
- [62] M. Buret, A.V. Uskov, J. Dellinger, N. Cazier, M.-M. Mennemanteuil, J. Berthelot, I.V. Smetanin, I.E. Protsenko, G. Colas-Des-Francs, A. Bouhelier, Spontaneous Hot-Electron Light Emission from Electron-Fed Optical Antennas, Nano Letters, 15 (2015) 5811-5818.
- [63] H. Park, A.K.L. Lim, A.P. Alivisatos, J. Park, P.L. Mceuen, Fabrication of metallic electrodes with nanometer separation by electromigration, Applied Physics Letters, 75 (1999) 301-303.
- [64] J.B. Herzog, M.W. Knight, Y. Li, K.M. Evans, N.J. Halas, D. Natelson, Dark Plasmons in Hot Spot Generation and Polarization in Interelectrode Nanoscale Junctions, Nano Letters, 13 (2013) 1359-1364.

- [65] G. Platero, R. Aguado, Photon-assisted transport in semiconductor nanostructures, Physics Reports, 395 (2004) 1-157.
- [66] S. Kohler, J. Lehmann, P. Hanggi, Driven quantum transport on the nanoscale, Physics Reports, 406 (2005) 379-443.
- [67] J. Tucker, Quantum limited detection in tunnel junction mixers, IEEE Journal of Quantum Electronics, 15 (1979) 1234-1258.
- [68] M.M.A. Yajadda, K.-H. Müller, D.I. Farrant, K. Ostrikov, Partial rectification of the plasmon-induced electrical tunnel current in discontinuous thin gold film at optical frequency, Applied Physics Letters, 100 (2012) 211105.
- [69] A.V. Bragas, S.M. Landi, O.E. MartíNez, Laser field enhancement at the scanning tunneling microscope junction measured by optical rectification, Applied Physics Letters, 72 (1998) 2075-2077.
- [70] M.M. Mennemanteuil, M. Buret, G. Colas-Des-Francs, A. Bouhelier, Optical rectification and thermal currents in optical tunneling gap antennas, Nanophotonics, 11 (2022) 4197-4208.
- [71] X. Chen, M. Roemer, L. Yuan, W. Du, D. Thompson, E. Del Barco, C.A. Nijhuis, Molecular diodes with rectification ratios exceeding 105 driven by electrostatic interactions, Nature Nanotechnology, 12 (2017) 797-803.
- [72] D. Thompson, C.A. Nijhuis, Even the Odd Numbers Help: Failure Modes of SAM-Based Tunnel Junctions Probed via Odd-Even Effects Revealed in Synchrotrons and Supercomputers, Accounts of Chemical Research, 49 (2016) 2061-2069.

- [73] C.A. Nijhuis, W.F. Reus, J.R. Barber, M.D. Dickey, G.M. Whitesides, Charge Transport and Rectification in Arrays of SAM-Based Tunneling Junctions, Nano Letters, 10 (2010) 3611-3619.
- [74] Q. Van Nguyen, Controlling Rectification in Metal–Molecules–Metal Junctions Based on 11-(Ferrocenyl) Undecanethiol: Effects of the Electronic Coupling Strength, The Journal of Physical Chemistry C, 126 (2022) 6405-6412.
- [75] A. Lombardi, A. Demetriadou, L. Weller, P. Andrae, F. Benz, R. Chikkaraddy, J. Aizpurua, J.J. Baumberg, Anomalous Spectral Shift of Near- and Far-Field Plasmonic Resonances in Nanogaps, ACS Photonics, 3 (2016) 471-477.
- [76] M. Yang, M.S. Mattei, C.R. Cherqui, X. Chen, R.P. Van Duyne, G.C. Schatz, Tip-Enhanced Raman Excitation Spectroscopy (TERES): Direct Spectral Characterization of the Gap-Mode Plasmon, Nano Letters, 19 (2019) 7309-7316.
- [77] M.M.A. Yajadda, K.-H. Müller, K. Ostrikov, Effect of Coulomb blockade, gold resistance, and thermal expansion on the electrical resistance of ultrathin gold films, Physical Review B, 84 (2011).
- [78] P. Zolotavin, C. Evans, D. Natelson, Photothermoelectric Effects and Large Photovoltages in Plasmonic Au Nanowires with Nanogaps, The Journal of Physical Chemistry Letters, 8 (2017) 1739-1744.
- [79] M.-M. Mennemanteuil, G. Colas-Des-Francs, M. Buret, A. Dasgupta, A. Cuadrado, J. Alda, A. Bouhelier, Laser-induced thermoelectric effects in electrically biased nanoscale constrictions, Nanophotonics, 7 (2018) 1917-1927.

- [80] S. Zhou, X. Guo, K. Chen, M.T. Cole, X. Wang, Z. Li, J. Dai, C. Li, Q. Dai, Optical-Field-Driven Electron Tunneling in Metal–Insulator–Metal Nanojunction, Advanced Science, 8 (2021) 2101572.
- [81] H. Chalabi, D. Schoen, M.L. Brongersma, Hot-Electron Photodetection with a Plasmonic Nanostripe Antenna, Nano Letters, 14 (2014) 1374-1380.
- [82] G. Aguirregabiria, D.C. Marinica, R. Esteban, A.K. Kazansky, J. Aizpurua, A.G. Borisov, Role of electron tunneling in the nonlinear response of plasmonic nanogaps, Physical Review B, 97 (2018).
- [83] C.A. Reynaud, D. Duché, J.-J. Simon, E. Sanchez-Adaime, O. Margeat, J. Ackermann, V. Jangid, C. Lebouin, D. Brunel, F. Dumur, D. Gigmes, G. Berginc, C.A. Nijhuis, L. Escoubas, Rectifying antennas for energy harvesting from the microwaves to visible light: A review, Progress in Quantum Electronics, 72 (2020) 100265.
- [84] F. Niroui, A.I. Wang, E.M. Sletten, Y. Song, J. Kong, E. Yablonovitch, T.M. Swager, J.H. Lang, V. Bulović, Tunneling Nanoelectromechanical Switches Based on Compressible Molecular Thin Films, ACS Nano, 9 (2015) 7886-7894.